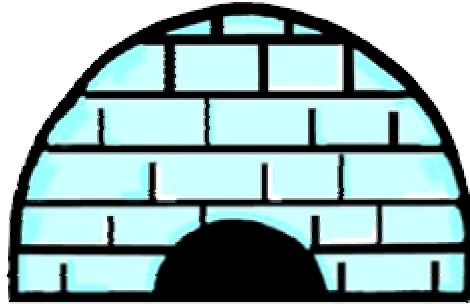


# How Warm is an Igloo?



**BEE453**  
**Spring 2003**

**Rich Holihan**  
**Dan Keeley**  
**Daniel Lee**  
**Powen Tu**  
**Eric Yang**

## HOW WARM IS AN IGLOO

Rich Holihan, Dan Keeley, Daniel Lee, Powen Tu, Eric Yang

*BEE 453  
Spring 2003*

### **Executive Summary**

Homeostasis maintains the human body temperature within a few degrees of 37°C. However, in severe environments, such as a harsh winter blizzard, the body will not be able to maintain a 37°C temperature without the aid of clothes, shelter, and sources of heat. We find the Igloo, a shelter made of ice and snow, a very interesting means of maintaining body temperature. In this project, we have created a mesh of the Igloo system in GAMBIT and ran simulations in FIDAP to examine temperature variation and air flow inside of the igloo, when the human body is the only source of heat. In the steady state temperature profile obtained, areas of highest temperature were located directly around and above the human, and close to the top of the igloo, the temperature was 289K. The areas of lowest temperature were around 266 K, located at the bottom of the igloo farthest from the human. Natural convection caused the velocity of the air in the igloo to range from 0 to 9mm/s. The FIDAP analysis did not take into account radiative heat transfer, so a separate analysis was done, which revealed that there is considerable heat transfer through radiation in an igloo.

## **Introduction**

In extremely cold temperatures, humans use most of the food ingested directly to generate heat. However, we are rather ill equipped for the intense cold, and heat generation by metabolism can easily become inadequate in maintaining a healthy body temperature. Without our warm jackets and heaters, humans can die of lowered body temperature within 20 minutes at a temperature of  $0^{\circ}\text{C}$ [1]. We need efficient means of protecting ourselves from the cold in order to survive in a harsh and unforgiving winter.

The Igloo is a domed snow house often associated with the Inuit, the native inhabitants of the Canadian Arctic. Igloos are relatively easy to construct, made from materials found in abundance: snow and ice. Blocks of ice are formed into the dome shape, “glued” together by snow. To prevent excessive amount of snow and wind from coming in, a sunken entrance is typically constructed, along with a raised sleeping platform covered with fur for comfort and warmth[2]. The igloo is an ingenious invention, very effective in keeping people warm. The question is: how?

The human body can lose heat in many ways, including radiation, conduction, convection, evaporation and even respiration. The igloo is a means to reduce heat loss by wind convection and by moisture from precipitation. With winds recorded up to hundreds of miles per hour, convection becomes a significant source of heat loss. Although moisture may not seem too threatening, hypothermia can occur at temperatures as high as  $4^{\circ}\text{C}$  if the body is chilled by sweat, rain, snow or other sources. Therefore, the Igloo does not provide heat, but rather, it preserves the heat generated by the body.

## **Project Design**

### *(I) Design Objectives*

- (a) To find the temperature distribution within an igloo at steady state.
- (b) To examine air flow within an igloo at steady state.

### *(II) Assumptions*

By steady state, we mean that the heat lost from the human body equates to the heat given to the inner igloo wall, as well as to the heat leaving the outer igloo wall. In doing so, a list of assumptions have been made in order to model the real-life situation (Please refer to Appendix A for input parameters):

- Body insulated from the snow on the ground
- Convection due to wind out side is negligible – only small air hole is present for oxygen and entrance is blocked.
- Human subject is not wearing any clothing, and the outer human body temperature is at 37 degrees Celsius, with direct conduction from skin to air.
- Constant ambient temperature outside.

- Constant properties – no significant melting of igloo or snow on the ground.
- Igloo wall is made up of compressed snow with 0% porosity.
- Our geometry model is axi-symmetric. Please refer to problem schematic (Figure 1).

*(III) Problem Schematic*

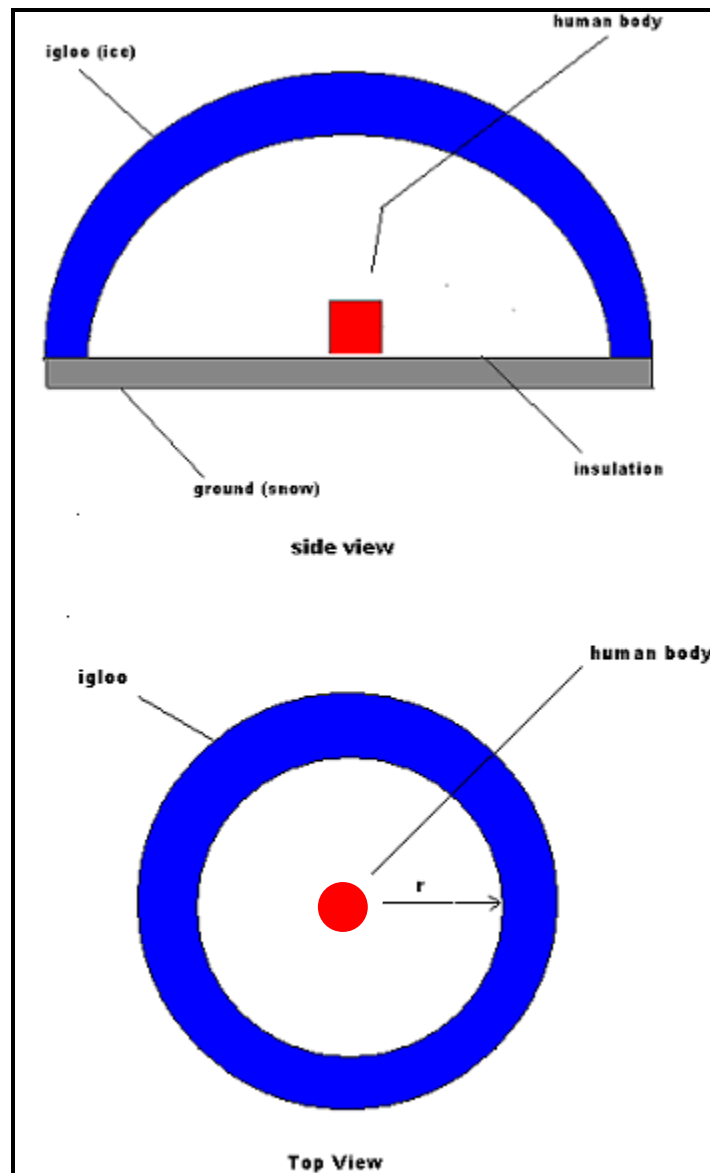


Figure 1. Igloo Schematic

*(IV) Importance of problem*

It is important to examine the inner igloo thermal conditions to see how comfortable the human being is inside, and if it is, our model can provide a basis to further expand into more complicated problems in the future, such as the duration to reach a steady state, comfortable environment.

*(V) Preview of report organization*

In this report, we will be presenting the temperature contours and the air velocity vectors due to thermal expansion within the igloo after steady state has been reached. These results and their sensitivity analysis are all obtained from the computer simulation within FIDAP program. For individual input property and geometry parameters, as well as mesh generated from GAMBIT, that are used in the simulation, please refer to Appendices.

## Results and Discussion

### *(I) Qualitative Description*

Within the igloo a naked human body generates heat by metabolism. This heat maintains a person's body temperature at 310 Kelvin. This heat is lost through a person's skin by conduction, convection and radiation. Heat transfer to surrounding air causes its temperature to rise and as a result density decreases. The effect of buoyancy pushes the warmer air towards the top of the igloo against gravity, while the cooled air near the ice surface of the igloo condenses and flows downward. This creates the circulating flow of convection that is depicted in Figure 2. It can be seen from the temperature profile (Figure 3), the air in contact with the skin surface reaches a temperature of 310K, and the nearby air reaches a temperature of approximately 290K. Due to the rising warm air, the temperature above the human is much warmer than other sections of the igloo. The edges of the igloo remain very cold at a temperature of approximately 273K. According to the velocity profile (Figure 4) we see that the air flows the fastest directly above the human at a velocity of approximately 9mm/s. Near the edges, the velocity ranges from 1mm/s to 2mm/s. The air in mid range flowed at approximately 5mm/s. The greatest velocity in the region above the human makes sense, as it matches with the convective heat flow region observed in the temperature profile. A few unusually large velocities were found at the axis of rotation. These velocities were a result of  $1/r$  coefficients in the governing equation. As  $r$  approaches zero the respective velocities increase to dramatic amounts. An error of this nature can be minimized by utilizing smaller iterations or higher mesh densities.

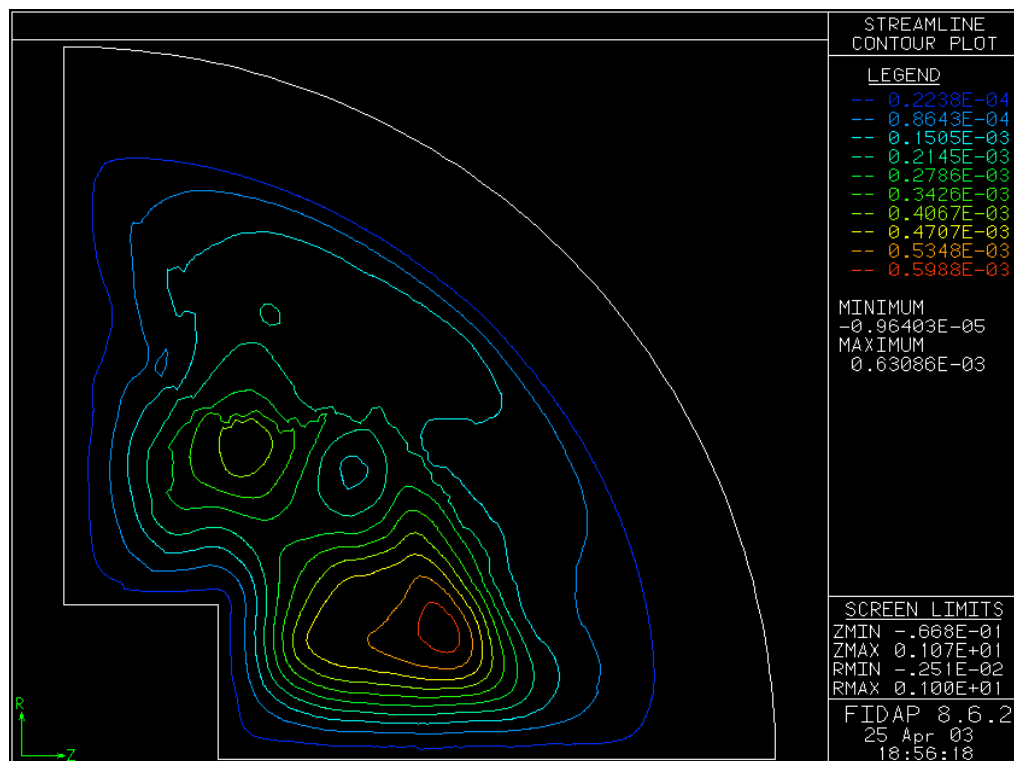


**Figure 2. Streamlines at 310K**

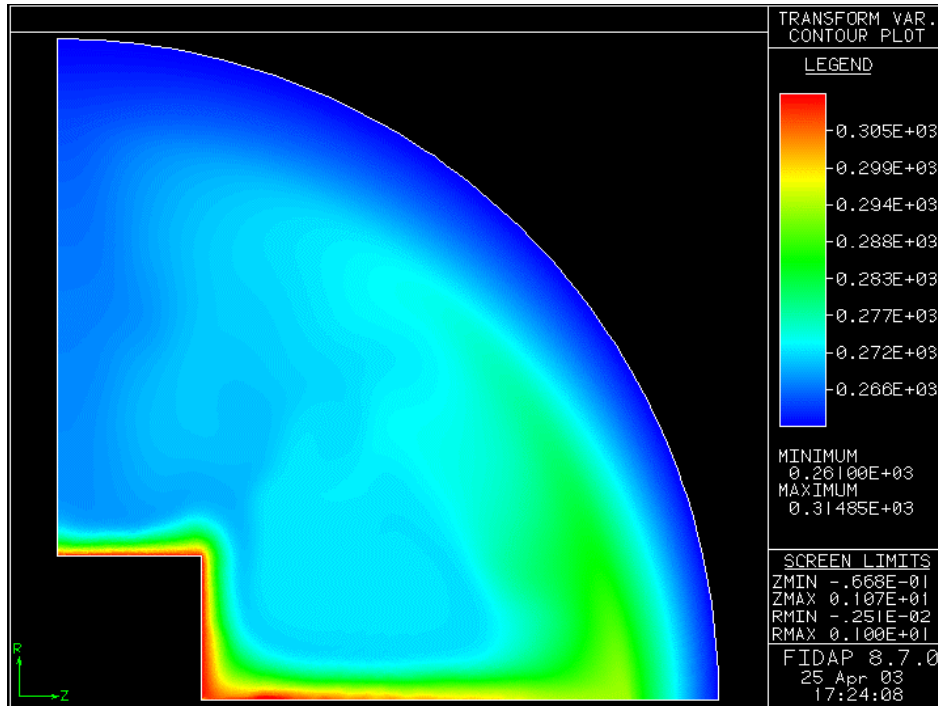


Figure 3. Temperature profile at 310K

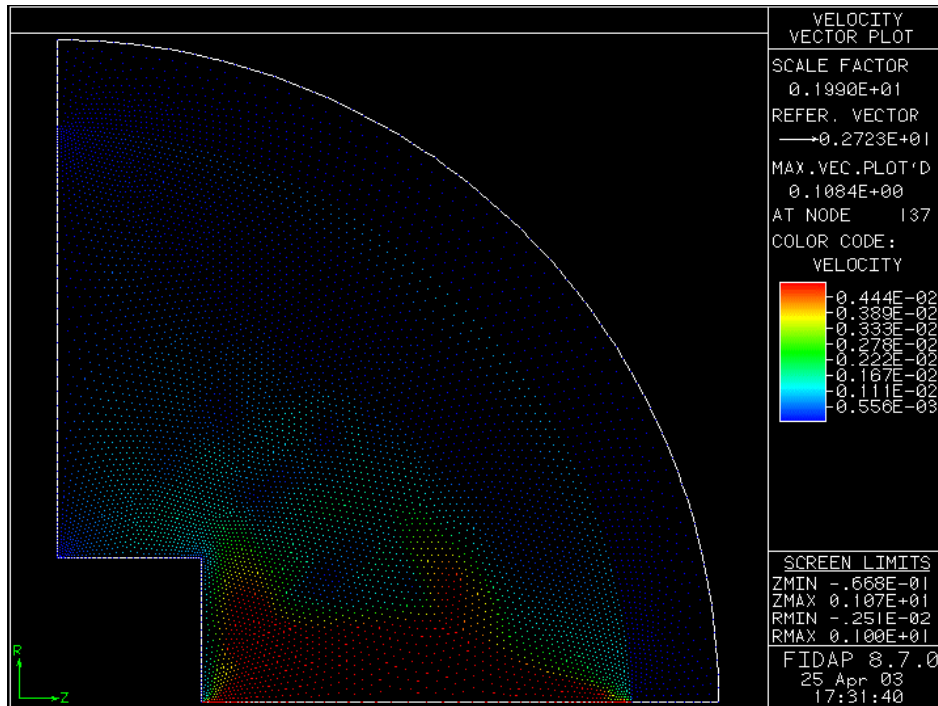


Figure 4. Velocity vector plot at 310K

When running the simulation, many manual iterations were done starting with a lower Raleigh number, so the solution would converge. When starting immediately with a high Raleigh number, the solution does not converge. Hence, the temperature contour is not realistic (Figure 1C). At a low Raleigh number, the viscosity is high and the temperature contour looks very similar to the results due to conduction (Figure 2C). These results are expected because at high viscosity, the air would be less likely to move, and heat transfer would primarily take place through conduction. As the Raleigh number is gradually increased, the effects due to convection are more clearly observed (Figures 3C and 4C). These results are also expected, as the lower viscosity values allow the air to move more freely and flow due to buoyancy, and natural convection effects are more dominant.

### *(II) Sensitivity Analysis*

The human inside the igloo was initially assumed to be naked with a body temperature of 310K. In more realistic conditions, the human would be wearing clothes, and the surface temperature should be lower at around 300K. For the sensitivity analysis, the boundary conditions of top human and side human were changed from 310K to 300K. The results show a similar velocity profile (Figures 9C and 10C) and similar streamlines (Figures 7C and 8C). From the temperature contour (Figures 5C and 6C), however, we can see that for the naked human model, there is slightly more temperature penetration towards the top of the igloo.

### *(III) Heat loss due to Radiation and Convection*

The calculated heat loss due to radiation is 490.64W, while the heat loss due to convection obtained from FIDAP is 59.84W. Literature shows that total heat loss of a human body should be approximately 50% convection and 50% radiation with negligible effect from conduction [9]. From our results, however, we have much less heat flux due to convection compared to the calculated value of radiation. Although unexpected at first, these results do make sense. Heat loss due to convection varies greatly with air movement, while radiation is independent of this movement. Inside the igloo, the air movement is caused only by the convection due to thermal gradient, and the air velocity is on the order of few millimeters per second. Therefore, it is not surprising that the heat flux due to convection is much less than the heat flux due to radiation. We believe that the 50/50 convection to radiation ratio applies only in conditions in which there is significant wind velocity and is not true for a case in which natural convection is the only source of air movement.

Considering both radiation and convective heat transfer we expect our final igloo temperature to be between 283-288 K. This is consistent with data found in “*The intriguing physics inside an Igloo*” (Wilson, 2001).

Equation used to calculate radiation:

$$Q_b/t = \epsilon \sigma A_b (T_b^4 - T_a^4) = 490.64W$$

Where:

$\epsilon_{\text{human}} = \text{emissivity constant} = 0.97 \text{ for human skin [10]}$

$\epsilon_{\text{ice}} = 0.95 \text{ at } 273\text{K [10]}$

$\sigma = \text{Stefan-Boltzmann constant} = 5.67 \times 10^{-8} \text{ W / m}^2 \text{ K}^4$

$A_b = \text{Surface Area of average adult male} = 160\text{m}^2$

$T_b = \text{body temperature} = 310\text{K}$

$T_a = \text{average temperature of igloo inner wall} = 271\text{K}$

### **Conclusions and Design Recommendations**

We have obtained the temperature and air flow profiles as stated in our design objectives. The air temperature reaches 310K near the skin surface, while the air above the human body reaches around 290K. These temperatures are acceptable values for human survival. However, the majority of the air does not heat up beyond 275K. This result may be primarily due to the fact that we did not incorporate radiation into the FIDAP analysis. Our calculations show that radiation causes considerable heat loss from the human, which should result in higher air temperature overall in real life situations. Our sensitivity analysis shows that with clothes on, air temperature within the igloo is lower, but there is no significant change in air flow patterns.

Our model has been simplified to limit the scope of our project. Some modifications, as such, can be made to improve the accuracy of our model. For instance, we assumed a constant human body temperature, but it is likely that the temperature will drop as the body loses heat to the air. In reality, there will most likely be other heat sources within the igloo, such as an oil lamp. In addition, we only considered heat loss out of the system through the outer wall of the igloo. Heat could also have been lost through the ground and air holes in the igloo wall (and even the door).

Overall, our model provided a reasonable study towards the temperature and velocity profiles within an igloo. In other words, a human being, naked as in our model, will be relatively comfortable in an igloo that has thermal conditions similar to our descriptions. In this case, the person would not have to invest in other insulating devices or heat sources to live in an igloo. Since we are modeling an already existing apparatus, cost considerations are not important in our analysis. That is, materials considered in our model such as snow and ice do not require cost considerations, especially in the North Pole and Alaskan regions. However, if we were to perform this experiment here in Ithaca and we did not want to wait for winter, we would have to make our own snow. A top of the line snow block maker will cost us approximately \$7,900 from Southern Snow MFG. Inc.

**Appendix A: Mathematical Statements of the Problem**

*(I) Geometry.*

In order to make our model more realistic, an axis-symmetric geometry was used calculate the solution. This model is more realistic because this way, we can analyze and simulate the entire igloo, instead of a half igloo slice from the 2-D model. An axis-symmetric schematic of our igloo is shown in Figure 1A, with geometry and boundary condition values. Human body generates heat within the igloo, and while the human body is sitting on the ground, it is modeled as a square. The dimensions are obtained form [3].

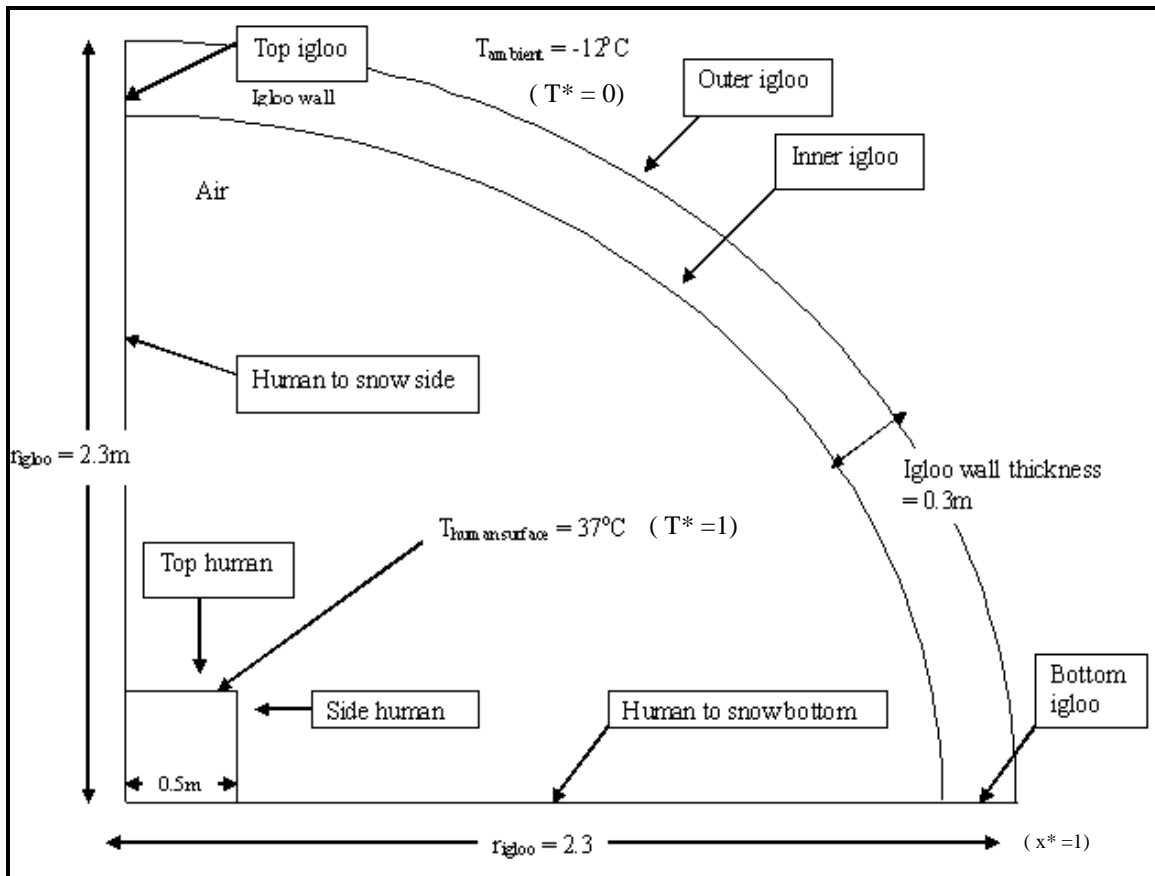


**Figure1A. Igloo geometry and Boundary Conditions\*\***

\*\* for T\*, x\* calculations, refer to appendices.

Since we are modeling the igloo as an axis-symmetric geometry, the coordinates are now in cylindrical aspect. Please refer to Figure 2A.

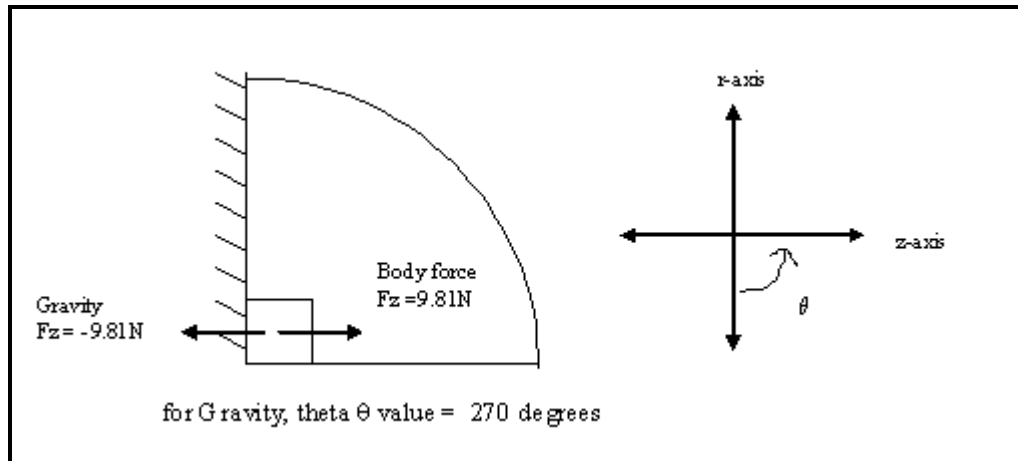


Figure 2A. Cylindrical coordinates and angle values for our model

## (II) Governing Equations and Boundary Conditions

Since we are trying to obtain the temperature profile within the igloo, we need the Energy equation (1) in cylindrical coordinates for our design objectives [4] In addition, we need the Momentum equation (2) in order to analyze natural convection within the igloo due to the change in temperature of the air. The Governing Equations are

Energy Equation:

Cylindrical

$$\frac{k}{\rho c_p} \left[ \frac{1}{r} \frac{\partial}{\partial r} \left( r \frac{\partial T}{\partial r} \right) + \frac{1}{r^2} \left( \frac{\partial^2 T}{\partial \theta^2} \right) + \frac{\partial^2 T}{\partial z^2} \right] + \frac{Q}{\rho c_p} = \frac{\partial T}{\partial t}$$

Explanations:

1. No heat generation (human heat generation is accounted for by surface temperature)
2. Steady state solution
3. No variation with respect to  $\Phi$ -axis

Momentum Equation:

*r*-component

$$\rho \left( \frac{\partial v_r}{\partial t} + v_r \frac{\partial v_r}{\partial r} + \frac{v_\theta}{r} \frac{\partial v_r}{\partial \theta} - \frac{v_\theta^2}{r} + v_z \frac{\partial v_r}{\partial z} \right) = -\frac{\partial p}{\partial r}$$

$$+ \mu \left( \frac{\partial}{\partial r} \left( \frac{1}{r} \frac{\partial}{\partial r} (r v_r) \right) + \frac{1}{r^2} \frac{\partial^2 v_r}{\partial \theta^2} - \frac{2}{r^2} \frac{\partial v_\theta}{\partial \theta} + \frac{\partial^2 v_r}{\partial z^2} \right) + \rho g_r$$

*θ*-component

$$\rho \left( \frac{\partial v_\theta}{\partial t} + v_r \frac{\partial v_\theta}{\partial r} + \frac{v_\theta}{r} \frac{\partial v_\theta}{\partial \theta} + \frac{v_r v_\theta}{r} + v_z \frac{\partial v_\theta}{\partial z} \right) = -\frac{1}{r} \frac{\partial p}{\partial \theta}$$

$$+ \mu \left( \frac{\partial}{\partial r} \left( \frac{1}{r} \frac{\partial}{\partial r} (r v_\theta) \right) + \frac{1}{r^2} \frac{\partial^2 v_\theta}{\partial \theta^2} + \frac{2}{r^2} \frac{\partial v_r}{\partial \theta} + \frac{\partial^2 v_\theta}{\partial z^2} \right) + \rho g_\theta$$

*z*-component

$$\rho \left( \frac{\partial v_z}{\partial t} + v_r \frac{\partial v_z}{\partial r} + \frac{v_\theta}{r} \frac{\partial v_z}{\partial \theta} + v_z \frac{\partial v_z}{\partial z} \right) = -\frac{\partial p}{\partial z}$$

$$+ \mu \left( \frac{1}{r} \frac{\partial}{\partial r} \left( r \frac{\partial v_z}{\partial r} \right) + \frac{1}{r^2} \frac{\partial^2 v_z}{\partial \theta^2} + \frac{\partial^2 v_z}{\partial z^2} \right) + \rho g_z$$

Explanations:

1. *θ*-component is not considered because there are no variations with respect to *θ*-axis
2. Steady state solution

Since we assumed steady state, no initial conditions are necessary. The boundary conditions are as follows:

1. Velocity of air flow = 0 at Top Human
2. Velocity of air flow = 0 at Side Human
3. Velocity of air flow = 0 at Human to snow side
4. Velocity of air flow = 0 at Human to snow bottom
5. Flux = 0 at Top Igloo
6. Flux = 0 at Bottom Igloo
7. Flux = 0 at Human to snow side
8. Flux = 0 at Human to snow bottom
9.  $T = 261\text{K}$ ,  $T^* = 0$  at Outer Igloo
10.  $T = 310\text{K}$ ,  $T^* = 1$  at Top Human
11.  $T = 310\text{K}$ ,  $T^* = 1$  at side Human

(III) All input parameters

**Table 1A. Properties**

Group	Properties	Values
Compressed snow properties	Specific Heat, Cp (T=300K, P=100kPa)	2090 J/Kg*K [6]
	Conductivity, k	0.3 J/s*m*K [3]
	Density, $\rho$	330 kg/m <sup>3</sup> [7]
Air (within igloo) properties at 0degrees C [8]	Density, $\rho$	1.292 kg/m <sup>3</sup>
	Specific Heat, Cp	1004.6 J/Kg*K
	Viscosity, $\mu$	0.18x10 <sup>-4</sup> Ns/m <sup>2</sup>
	Volume Expansion Coeff. $\beta$	0.0035 1/K
	Conductivity, k	0.025 W/m*K
Human Properties [3]	Width	0.5m
Igloo Dimensions [3]	Radius	2.0m
	Thickness	0.3m

(Note: numbers in brackets signify references.)

**Table 1B. Input parameters into GAMBIT and FIDAP**

Group	Parameters	Input Values
Igloo Dimensions $x^* = x/L$	SideHuman	0.5/2.3 = 0.217
	Top Human	0.5/2.3 = 0.217
	Human to snow side	2.0/2.3 = 0.870
	Human to snow bottom	2.0/2.3 = 0.870
	Top Igloo	0.3/2.3 = 0.130
	Bottom Igloo	0.3/2.3 = 0.130
Temperatures $T^* = (T - T_0) / (T_1 - T_0)$	Human	(310 - 261) / (310 - 261) = 1
	Outer Igloo	(261 - 261) / (310 - 261) = 0
Density** $\rho = \sqrt{(Ra/Pr)}$	Air	$\sqrt{(7.838 \times 10^{10} / 0.7233)} = 329187.55$
--	Gravity	1
--	Thermal Expansion	1
--	Conductivity	1
--	Viscosity	1
	Specific Heat (Cp=Pr)	0.7233

\*\*Density for snow is negligible because at low Pr, it is a solid, with high viscosity (Ra~0), which means no thermal air flow.

## Appendix B: FIDAP Commands

### *(I) FIDAP Input File and Explanations*

The igloo was modeled as an axis-symmetric quarter circle. Our goal was to determine the temperature profile and air flow in the igloo at steady state. Our problem definition also involved modeling the air inside the igloo as incompressible for simplicity. The non-linear parameter was used in this problem so that the convective terms could be included in the momentum and energy equations as is necessary to analyze the air flow in the igloo by natural convection. The fluid properties of the air were accepted to be Newtonian. Our natural convection is caused by temperature gradients. Warm air will have a slightly lower density than air cooler air and will rise. To take into account the variation in air density coupled with air temperature the buoyancy model was included in our problem definition as part of the momentum equation to determine the air flow.

A Rayleigh number was calculated in our problem to account for thermal loading that FIDAP calculates to simulate heat flow in association with air flow. Thermal loading for this problem is defined as the difference between the temperature of the human and the temperature of the outer wall. This loading cannot be applied in one step because the defining equations of the non-dimensional parameters are highly non-linear. As a result, to find convergence we were forced to solve several intermediate load cases with each solution becoming the initial iterate for solutions at the next case. We started out with a low Rayleigh number and ran the simulation. Once the FDPOST file was available from the first run, we renamed it to FDREST and restarted the simulation using the new set of data obtained from the FDREST file. To run the simulation using the FDREST file the execution parameter was changed from New Job to Restart. The procedure was repeated by increasing the Rayleigh number by a power of ten each time until the true Rayleigh number was reached. For the more detailed mesh, however, smaller incremental change in the Rayleigh number was necessary for the solution to converge. While the original mesh required approximately ten iterations, the detailed mesh required approximately thirty iterations.

The Newton-Raphson solution procedure was used since it has a higher rate of convergence than that of the default successive substitution method. FIDAP help manual indicates that the Newton-Raphson is the recommended solution procedure for small to moderate 2-D or axis-symmetric flow as is the case in the minute flow associated with natural convection in our igloo.

Since we modeled the air as incompressible even though it is realistically compressible we lowered the penalty for pressure to a value an order of magnitude smaller than the default value of  $1 \cdot 10^{-6}$ . In this way we reduced the constraints of the pressure variable in the momentum equation as it relates to an incompressible substance. Results were therefore more flexible with that of a compressible substance.

Entities “top igloo”, “bottom igloo”, “outer igloo”, “inner igloo”, “human to snow bottom”, “human to snow side”, “side human”, and “top human” were all set to type PLOT because they are simply references to be used in defining boundary conditions. PLOT type has no affect on analysis whatsoever.

Entity “igloo wall” was set to type SOLID because we modeled the igloo wall as a non-porous element and therefore there should be no air flow through it. As a SOLID

only the energy equation without the convective term will be solved reducing the energy equation to a pure diffusion equation in this region (see Figure 1A). This entity was also defined as SET 1 so that density, viscosity, specific heat, and conduction could be defined separately for the ice wall and the air inside the igloo. Values for these parameters can be found in Table....

Entity “air” was set to FLUID type. The FLUID keyword specifies that in this entity the buoyancy, continuity, and energy equations as defined in the problem command will be solved. Natural convection from temperature gradients will only be solved in this region (see Figure 1A). Entity “air” was defined as SET 2 to differentiate its properties from those of the igloo wall. Dimensionless values were inputted for parameters for set two as shown in Table 1B. The thermal expansion coefficient, air viscosity, and conductivity coefficient for entity “air” all had values of one because the Rayleigh number and the Prandtl number already take into account these properties true values. The specific heat was set to the Prandtl number while the value for density was set equal to the Rayleigh number. (See Appendix C).

Gravity was also a property that had a magnitude set to 1 because of dimensionless analysis. Gravity has a theta value of 270° because FIDAP assumes the default direction of gravity is downward or 0°. However, for an axi-symmetric problem such as our igloo the axis of symmetry is the bottom boundary of our igloo. So the side of our igloo as recognized by FIDAP is actually the bottom of the igloo and therefore the gravity direction must be adjusted 270 degrees in rotation to indicate the true gravitational force direction.

Our BCNODE boundary conditions were also subject to non-dimensional parameterization. The temperature of “outer igloo” was calculated to be 0 in non dimensional terms while the temperature of “side human” and “top human” were set to the non dimensional value of 1.

The velocity of air flow at “inner igloo”, “human to snow side”, “top human”, and “side human” were set to 0 because there is no velocity at the boundary walls because the boundaries are not considered part of the fluid. Also, the heat flux at “top igloo”, and “human to snow side” were set to 0 because we assumed that no heat was lost to the ground (top igloo and snow side are technically the igloo bottom and snow bottom of the model respectively). The heat flux for “bottom igloo” and “human to snow bottom” boundaries were set to 0 because these boundaries lie on the axis of symmetry.

FIDAP Input file:

*PROB (AXI-, INCO, STEA, LAMI, NONL, NEWT, MOME, FIXE, NOST, NORE, SING, BUOY)*

*PRES (PENA = 0.100000000000E-07, DISC)*

*EXEC (NEWJ)*

*SOLU (N.R. = 15, VELC = 0.100000000000E-02, RESC = 0.100000000000E-02,*

*ACCF = 0.000000000000E+00)*

*STRA (S.S. = 1)*

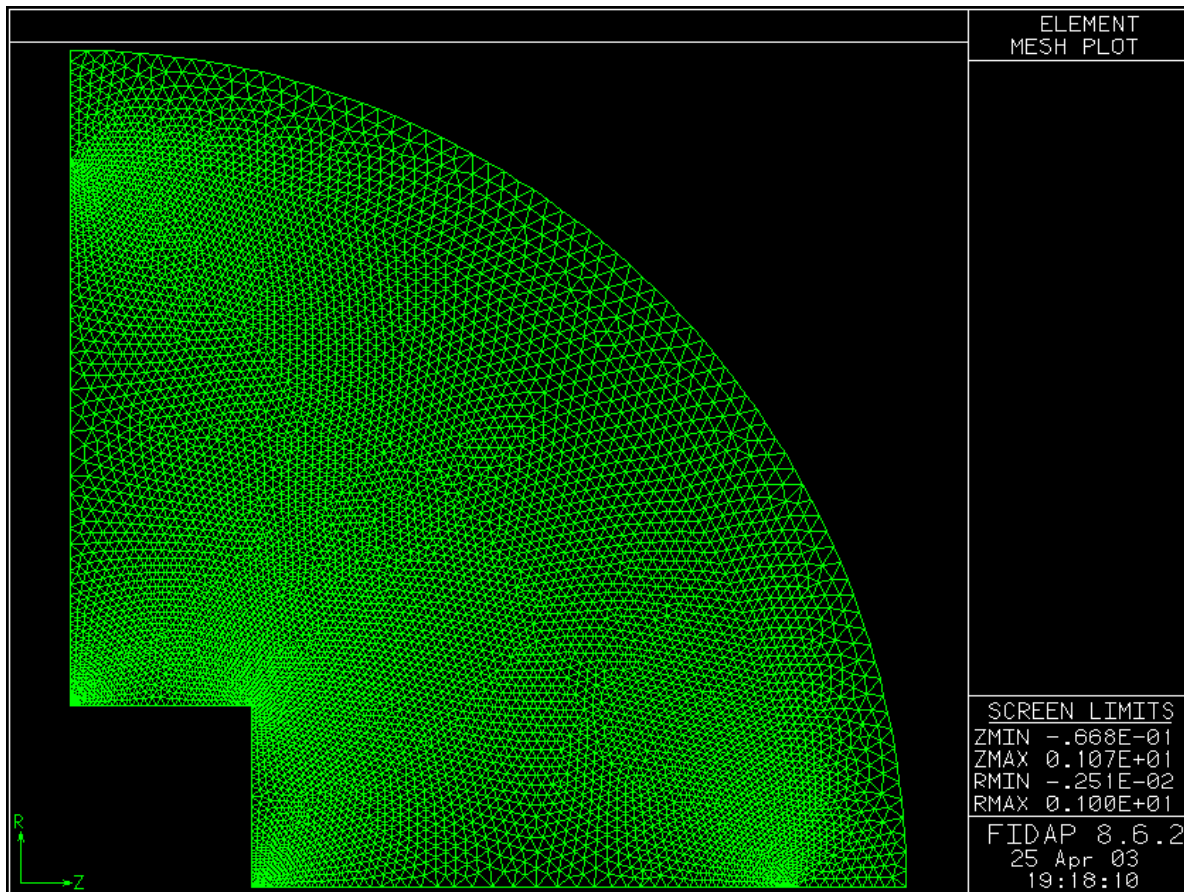
*GRAV (MAGN = 1.0, THET = 270.0, PHI = 0.000000000000E+00)*

*ENTI (NAME = "air", FLUI, MDEN = 2, MVIS = 2, MSPH = 2, MCON = 2)*

*ENTI (NAME = "igloo wall", SOLI, MDEN = 1, MSPH = 1, MCON = 1)*

*ENTI (NAME = "top igloo", PLOT)*

*ENTI (NAME = "bottom igloo", PLOT)*  
*ENTI (NAME = "outer igloo", PLOT)*  
*ENTI (NAME = "inner igloo", PLOT)*  
*ENTI (NAME = "human to snow bottom", PLOT)*  
*ENTI (NAME = "side human", PLOT)*  
*ENTI (NAME = "top human", PLOT)*  
*ENTI (NAME = "human to snow side", PLOT)*  
*DENS (SET = 1, CONS = 1.0)*  
*DENS (SET = 2, CONS = 329187.55)*  
*VISC (SET = 2, CONS = 1.0)*  
*SPEC (SET = 1, CONS = 2090.0)*  
*SPEC (SET = 2, CONS = 0.7233)*  
*COND (SET = 1, CONS = 1.0)*  
*COND (SET = 2, CONS = 1.0)*  
*VOLU (SET = 2, CONS = 1.0, REFT = 0.000000000000E+00)*  
*BCNO (TEMP, ENTI = "outer igloo", CONS = 0.000000000000E+00)*  
*BCNO (TEMP, ENTI = "side human", CONS = 1.0)*  
*BCNO (TEMP, ENTI = "top human", CONS = 1.0)*  
*BCNO (VELO, ENTI = "inner igloo", CONS = 0.000000000000E+00,*  
*X = 0.000000000000E+00, Y = 0.000000000000E+00, Z = 0.000000000000E+00)*  
*BCNO (VELO, ENTI = "top human", CONS = 0.000000000000E+00,*  
*X = 0.000000000000E+00, Y = 0.000000000000E+00, Z = 0.000000000000E+00)*  
*BCNO (VELO, ENTI = "human to snow side", CONS = 0.000000000000E+00,*  
*X = 0.000000000000E+00, Y = 0.000000000000E+00, Z = 0.000000000000E+00)*  
*BCNO (VELO, ENTI = "side human", CONS = 0.000000000000E+00,*  
*X = 0.000000000000E+00, Y = 0.000000000000E+00, Z = 0.000000000000E+00)*  
*BCFL (HEAT, ENTI = "top igloo", CONS = 0.000000000000E+00)*  
*BCFL (HEAT, ENTI = "bottom igloo", CONS = 0.000000000000E+00)*  
*BCFL (HEAT, ENTI = "human to snow bottom", CONS = 0.000000000000E+00)*  
*BCFL (HEAT, ENTI = "human to snow side", CONS = 0.000000000000E+00)*  
*END*

*(II) A Plot of the element mesh*

**Figure 1B. Original Mesh with 15,000 nodes**

Explanation of mesh:

The mesh (as shown in Figure 1B) is most detailed near the human surfaces because this is where the most significant changes in temperature occur. The velocity boundary conditions at the igloo walls are equal to zero. The velocity gradient in these regions is very important because of these boundary conditions. Therefore a double sided gradient was used in constructing nodes in order to get more detailed solutions in these important areas. This also saves computational time in the more central areas of the igloo.

*(III) Convergence of the solution and mesh refinement*

A more detailed mesh (Figure 2B) was created to determine the accuracy of our solution. The number of nodes was doubled from 15,000 to 30,000, with all other parameters and dimensions kept unchanged. While it took 10 iterations to obtain the final solution for the original mesh, the more detailed mesh required 35 iterations before the final solution could be obtained. The temperature profile, velocity vector plot and streamlines do not significantly change with the increase in node density (Figures 3B to

5B), and neither does the temperature plot for a chosen line in the igloo (Figure 6B(a)). A smoother curve is obtained for the more detailed mesh (Figure 6B(b)) in comparison to the original mesh (Figure 6B(c)), but this is expected as there are more points on the line to plot. It can thus be concluded that our solution is independent from our mesh.

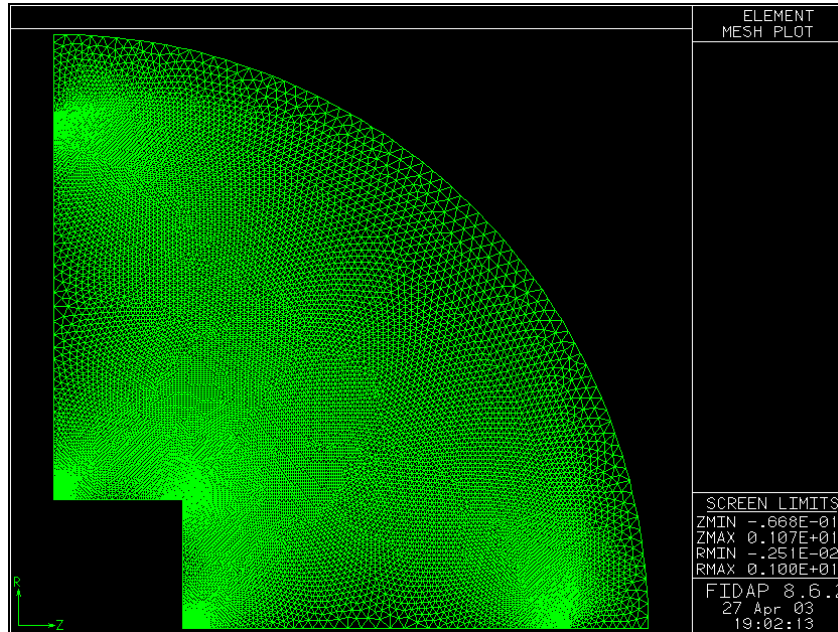


Figure 2B. Mesh with 30,000 nodes

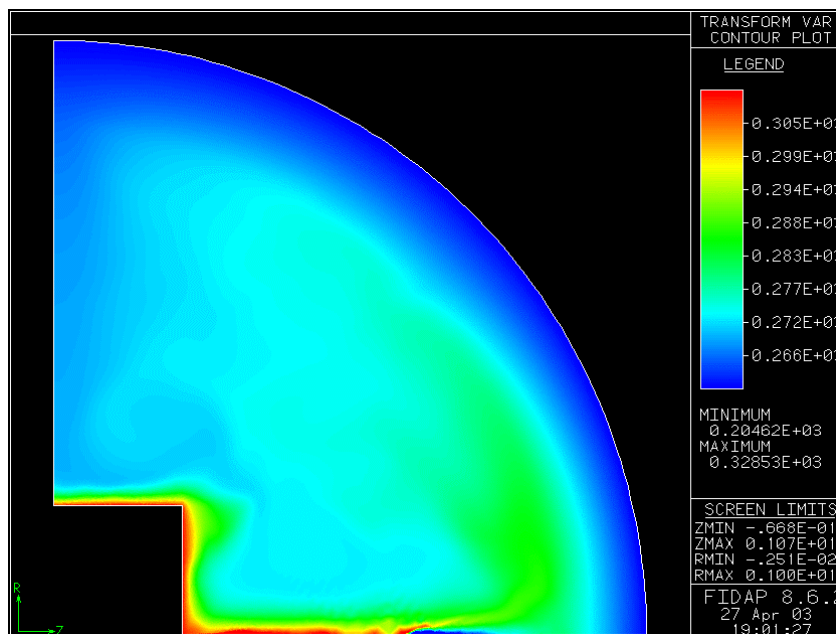


Figure 3B. Temperature profile for mesh with 30,000 nodes

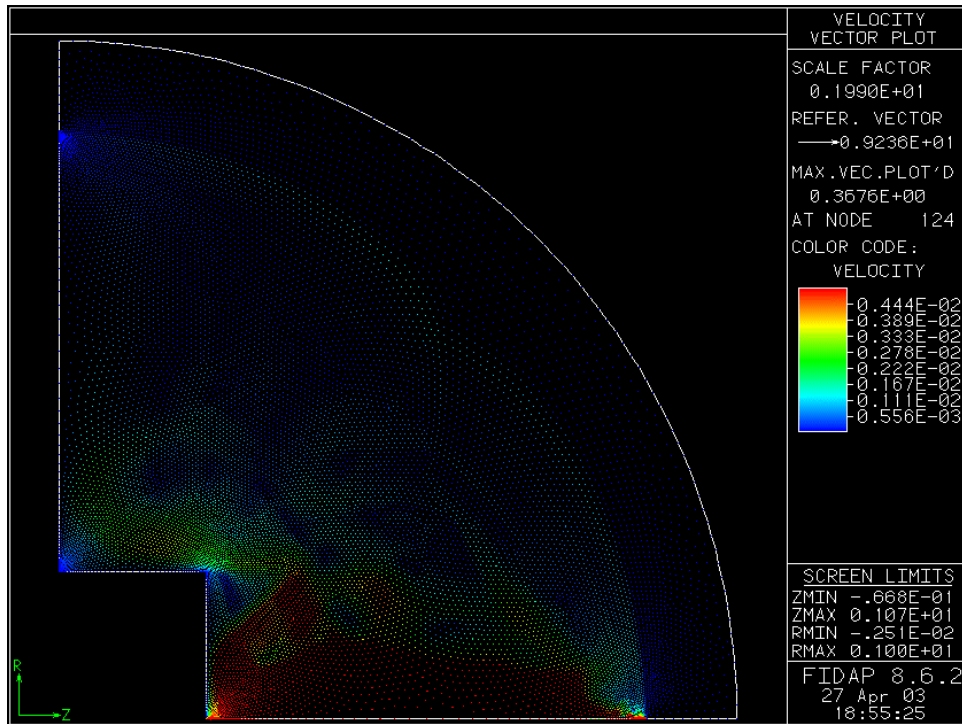


Figure 4B. Velocity vector plot for mesh with 30,000 nodes

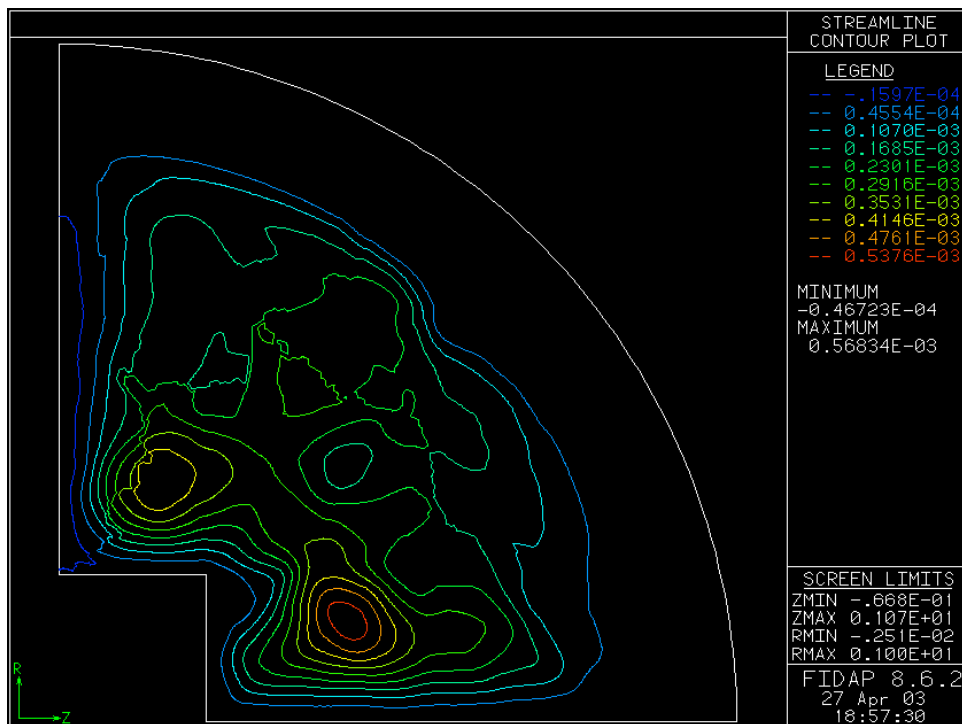


Figure 5B. Streamlines for mesh with 30,000 nodes

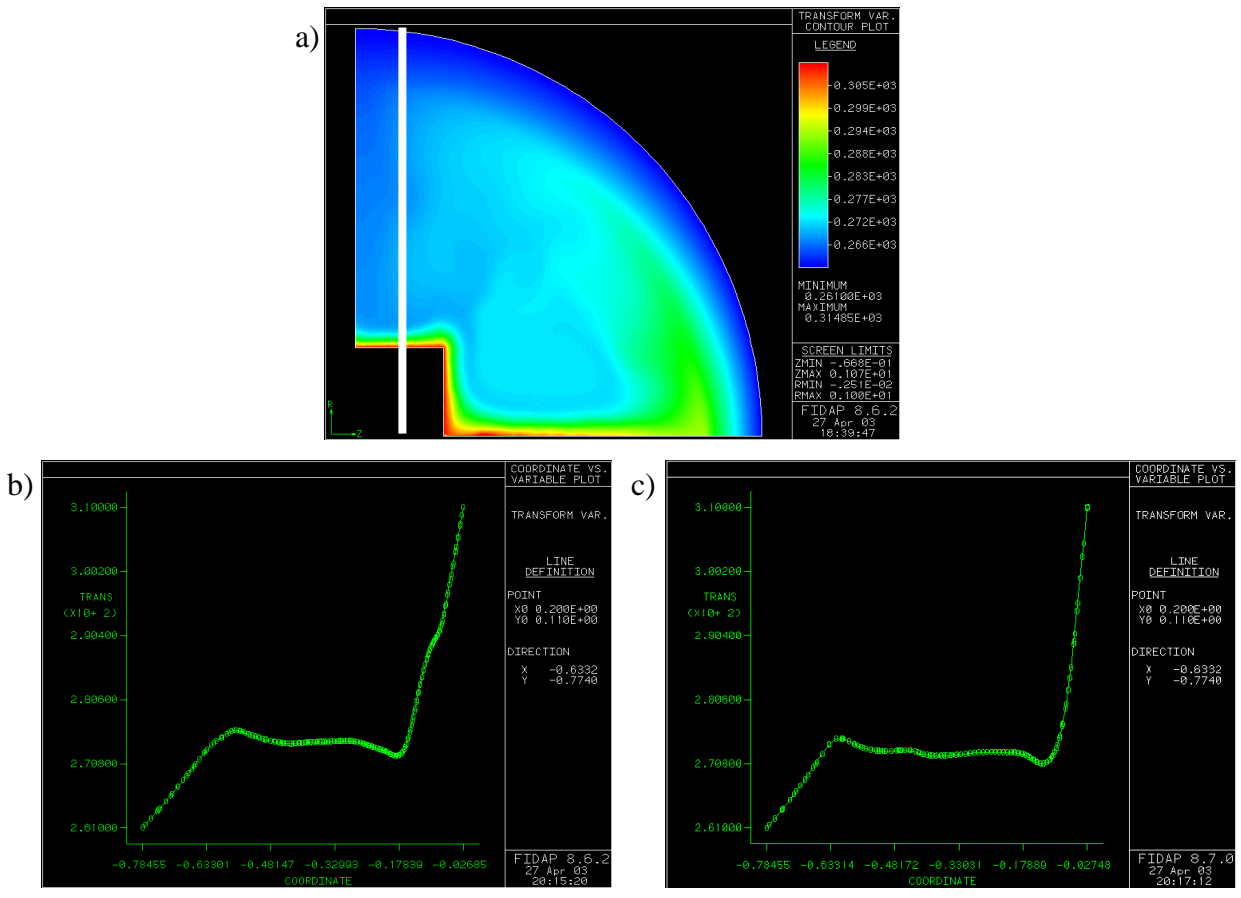
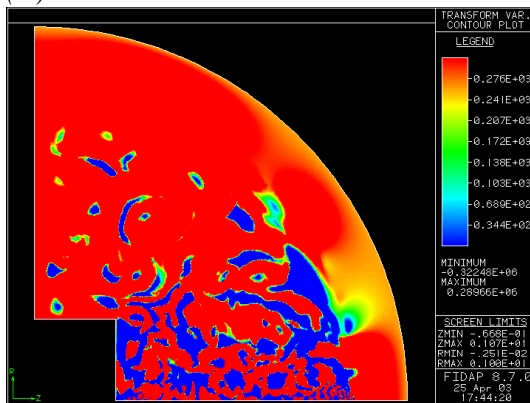


Figure 6B. Temperature plot for chosen line (a) Line chosen (b) 30,000 nodes (c) 15,000 nodes

**Appendix C: Other data, visuals and derivations**

**(A) Results**



**Figure 1C. Temperature contour without iterations. The solution does not converge.**

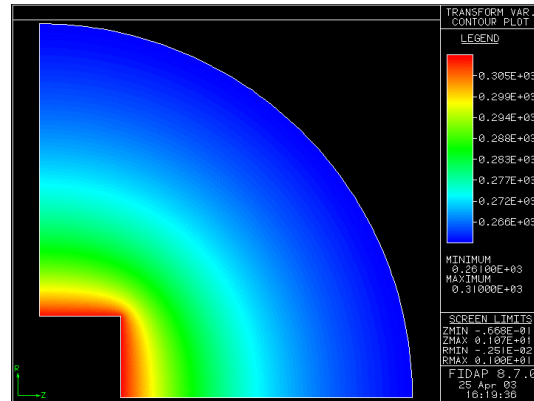


**Figure 2C. Temperature contour with high viscosity. (Low Raleigh number)**

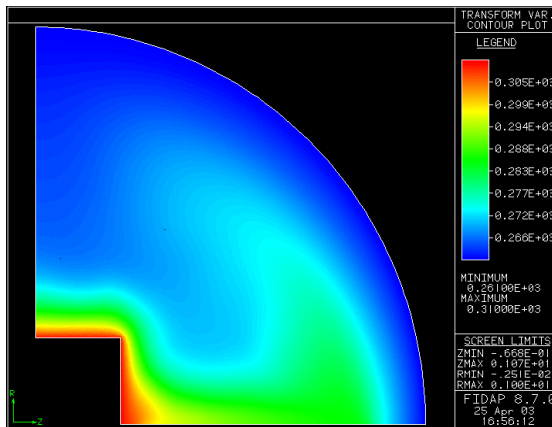


**Figure 3C. Temperature contour with higher Raleigh Number**

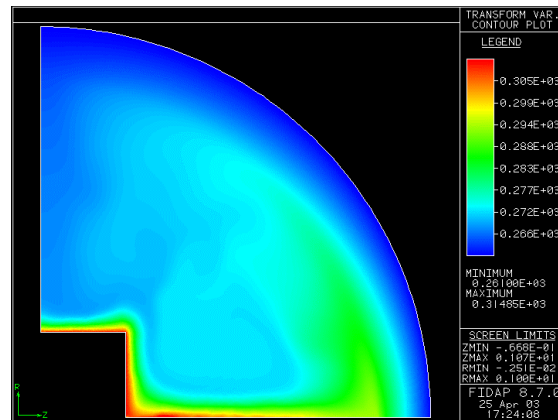


**Figure 4C. Temperature contour with true Raleigh number value (low air viscosity)**

**(B) Sensitivity Analysis**

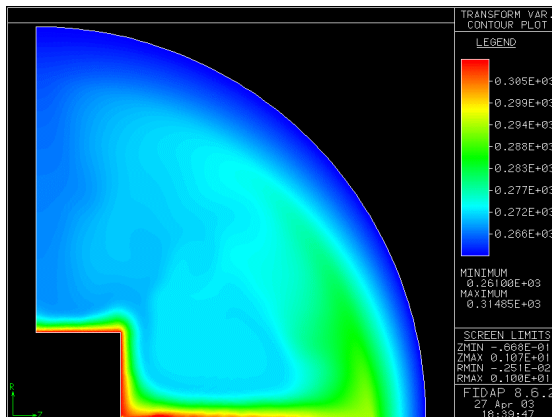


**Figure 5C. Temperature contour at 310K**

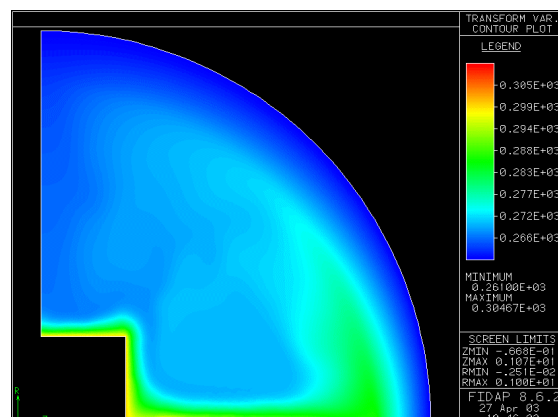


**Figure 6C. Temperature contour at 300K**

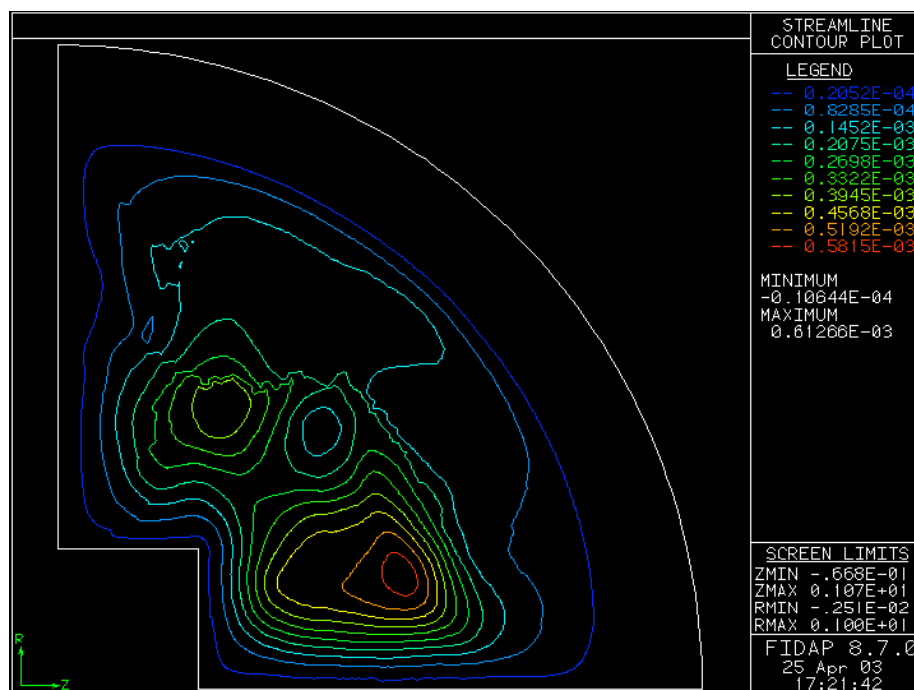


Figure 7C. Streamlines at 310K

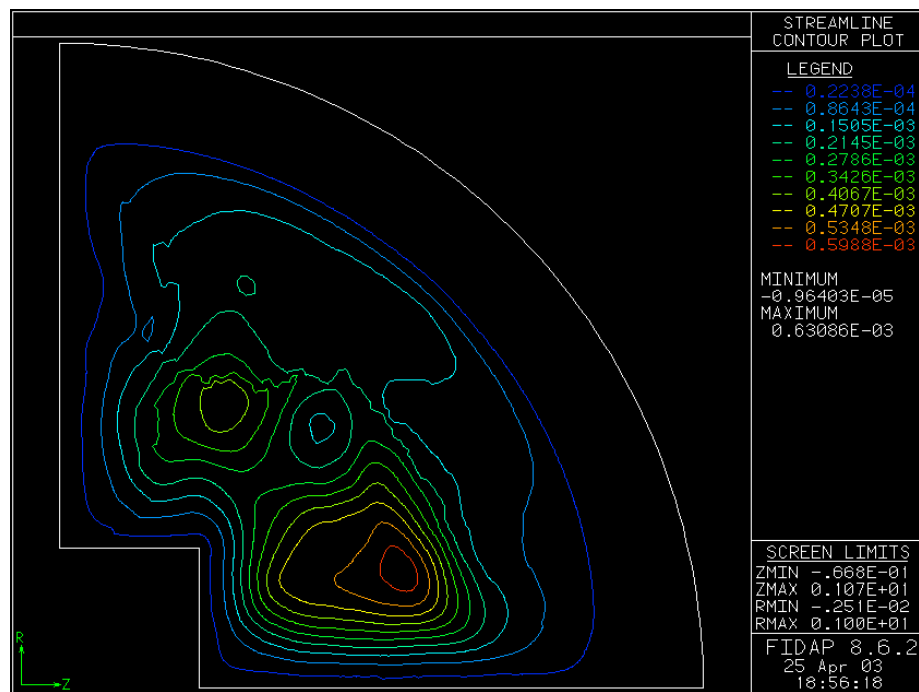


Figure 8C. Streamlines at 300K

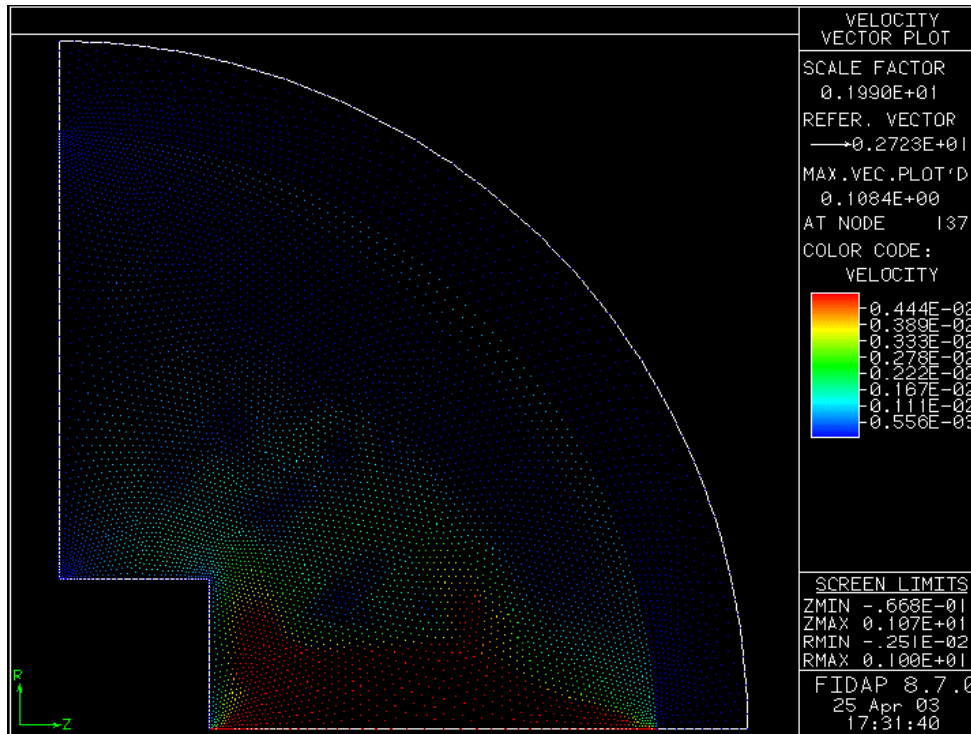


Figure 9C. Velocity vector plot at 310K

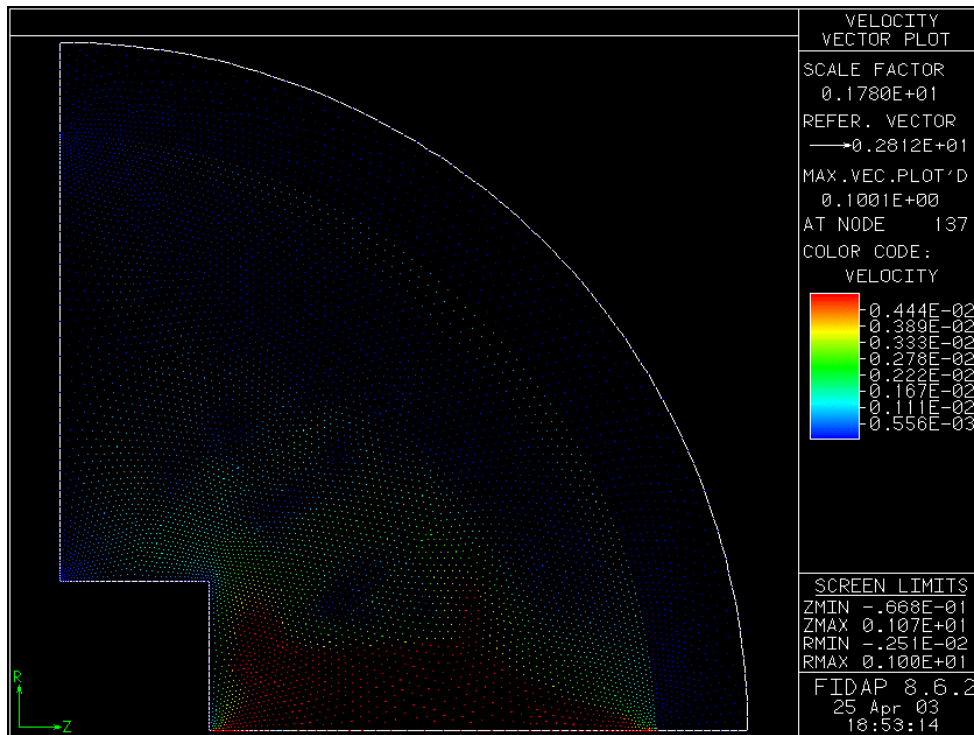


Figure 10C. Velocity vector plot at 300K

### *Dimensional Analysis*

(Derivations have been done in Cartesian Coordinates for simplicity. The actual coordinates used in the simulation are cylindrical coordinates)

Our Governing Equations in Cartesian Coordinates:

1.  $\nabla \cdot \mathbf{u} = 0$  (Mass conservation)
2.  $\rho c_p \mathbf{u} \cdot \nabla T = k \nabla^2 T$  (Energy conservation)
3.  $\rho \mathbf{u} \cdot \nabla \mathbf{u} = -\nabla p + \rho \mathbf{g} \beta(T-T_0) + \mu \nabla^2 \mathbf{u}$  (Momentum conservation)

where  $\mathbf{u}$  = velocity (m/s) vector

$T$  = temperature (K)

$\mu$  = viscosity (N-s/m<sup>2</sup>)

$c_p$  = specific heat (J/kg-K)

$k$  = conductivity (W/m-K)

$\beta$  = volume expansion coefficient (K<sup>-1</sup>)

$\rho$  = density (kg/m<sup>3</sup>)

$p$  = pressure (N/m<sup>2</sup>)

$\mathbf{g} = g \mathbf{e}$  = gravity (m/s<sup>2</sup>), where  $\mathbf{e}$  is a unit vector in the direction of the gravitational force.

The parameters in the governing equations are non-dimensionalized in order to simplify our problem, reduce the risks of large magnitude numbers that will off-lead FIDAP, and to define the parameters that have dominant physical phenomena.

In order to reduce the number of parameters, we define the following fixed parameters and new terms:

Fixed length =  $L$  (m)

Fixed Temperature =  $T_0$  (K) at some reference point

Reference velocity,  $U = (\alpha/L) * \sqrt{RaPr}$  (m/s)

Thermal diffusivity,  $\alpha = k / (\rho * c_p)$  (m<sup>2</sup>/s)

If we set  $\beta$  and  $\mathbf{g}$  equal to unity (1), their values will be weighted by the other dimensionless parameters that will be derived. Hence, the total number of parameters listed above is 10 ( $\mathbf{u}$ ,  $T$ ,  $\mu$ ,  $\alpha$ ,  $\beta$ ,  $\mathbf{g}$ ,  $L$ ,  $p$ ,  $U$ ) with 4 (Length(L), Time(s), Mass(kg), Temperature(K)) different dimensions total. According to the Buckingham Pi Theorem, there are

$$\begin{aligned}
 (\# \text{ parameters}) - (\# \text{ dimensions}) &= \text{minimum \# of dimensionless parameters} \\
 10 - 4 &= 6 \text{ total dimensionless parameters needed.}
 \end{aligned}$$

Let  $\Pi_n$  = dimensional parameters, where  $n = 1, 2, 3, \dots$ ,

By inspection,

$$\Pi_1 = \mathbf{u}^* = \mathbf{u} / U$$

$$\Pi_2 = T^* = (T - T_0) / (T_1 - T_0) \text{ where } T \text{ and } T_1 \text{ are temperatures at any arbitrary points}$$

and from algebraic manipulation:

$$\begin{aligned} \text{let } \Pi_3 = p^* &= p^w L^x \mu^y U^z \\ &= [MT^{-2} L]^w [L]^x [ML^{-1}T^{-1}]^y [LT^{-1}]^z \\ \text{where } M &= \text{mass} \\ T &= \text{Temperature} \\ L &= \text{Length} \end{aligned}$$

To make dimensionless, the sum of all dimensions must be 0:

$$\begin{aligned} M: & (1)w + (0)x + (1)y + (0)z = 0 \\ T: & (-2)w + (0)x + (-1)y + (-1)z = 0 \\ L: & (1)w + (1)x + (-1)y + (1)z = 0 \end{aligned}$$

After manipulation,

$w=1; x=1; y=-1; z=-1$ , which corresponds to:

$$\Pi_3 = p^* = p^1 L^1 \mu^{-1} U^{-1} = (pL)/(\mu U)$$

similarly, other Pi terms are developed:

$$\Pi_4 = x^* = x/L \text{ where } x \text{ represents the coordinates in the velocity vector term.}$$

$$\Pi_5 = \mu c_p / k = \text{Prandtl number (Pr)}$$

$$\Pi_6 = \rho \beta g (T_1 - T_2) L^3 / (\mu \alpha) = \text{Rayleigh Number (Ra)}$$

These dimensionless terms will be used to dimensionalize our governing equations. In doing so, we have to express the parameters in the equations with respect to their dimensionless terms (eg.  $\mathbf{u} = \mathbf{u}^* U$ )

Hence for the 1<sup>st</sup> governing equation, mass conservation, at steady state:

$$\nabla \cdot \mathbf{u} = 0 = \partial u / \partial x + \partial u / \partial y + \partial u / \partial z \quad (1a)$$

$$\text{where } \partial u = \partial u U, \text{ and } (\partial u / \partial x)U \quad (1b)$$

if we manipulate similarly for y, z coordinates to (1b), (1a) becomes:

$$\nabla \mathbf{u} = 0 = (\partial u / \partial x)U + (\partial u / \partial y)U + (\partial u / \partial z)U = U [\partial u / \partial x + \partial u / \partial y + \partial u / \partial z] \quad (1c)$$

$$\text{from (1b), bring U to LHS: } \nabla \mathbf{u} \Rightarrow \boxed{\nabla \mathbf{u}^* = 0} \quad (A)$$

For the 2<sup>nd</sup> governing equation, energy conservation, at steady state:

$$\rho c_p \mathbf{u} \cdot \nabla T = k \nabla^2 T \quad (2)$$

by expanding (2), we get:

$$\rho c_p \mathbf{u} \cdot [\partial T / \partial x + \partial T / \partial y + \partial T / \partial z] = k [\partial^2 T / \partial x^2 + \partial^2 T / \partial y^2 + \partial^2 T / \partial z^2] \quad (2a)$$

$$\text{where } \partial x^* = \partial x / L \\ \partial T^* = \partial T / (T_1 - T_0)$$

$$\text{hence } \partial T / \partial x = (\partial T^* / \partial x^*) [(T_1 - T_0) / L] \quad (2b)$$

$$\text{Similarly, } \partial T / \partial y = (\partial T^* / \partial y^*) [(T_1 - T_0) / L]; \partial T / \partial z = (\partial T^* / \partial z^*) [(T_1 - T_0) / L] \quad (2c)$$

Plugging (2b), (2c) into (2a), we get:

$$\rho c_p \mathbf{u} \cdot [(\partial T^* / \partial x^*) [(T_1 - T_0) / L] + \partial T^* / \partial y^* [(T_1 - T_0) / L] + (\partial T^* / \partial z^*) [(T_1 - T_0) / L]] = k [\partial^2 T / \partial x^2 + \partial^2 T / \partial y^2 + \partial^2 T / \partial z^2]$$

factoring out terms,

$$[\rho c_p \mathbf{u} (T_1 - T_0) / L] [\partial T^* / \partial x^* + \partial T^* / \partial y^* + \partial T^* / \partial z^*] = k [\partial^2 T / \partial x^2 + \partial^2 T / \partial y^2 + \partial^2 T / \partial z^2] \quad (2d)$$

$$\text{for } \partial^2 T^* / \partial x^{*2} = \partial (\partial T^* / \partial x^*) / \partial x^* \quad (2e)$$

plugging (2b) into (2e), we get:

$$\partial^2 T^* / \partial x^{*2} = \partial [(\partial T / \partial x) (L / (T_1 - T_0))] / \partial x^* = [\partial^2 T / \partial x^2] [L^2 / (T_1 - T_0)] \quad (2f)$$

and plugging (2f) into (2d), we get after some algebraic manipulation:

$$[\rho c_p \mathbf{u} (T_1 - T_0) / L] [\partial T^* / \partial x^* + \partial T^* / \partial y^* + \partial T^* / \partial z^*] = k [(T_1 - T_0) / L^2] [\partial^2 T^* / \partial x^{*2} + \partial^2 T^* / \partial y^{*2} + \partial^2 T^* / \partial z^{*2}]$$

or

$$[\rho c_p \mathbf{u} L][\partial T^*/\partial x^* + \partial T^*/\partial y^* + \partial T^*/\partial z^*] = k [\partial^2 T^*/\partial x^{*2} + \partial^2 T^*/\partial y^{*2} + \partial^2 T^*/\partial z^{*2}]$$

or

$$\rho c_p \mathbf{u} L \nabla T^* = k \nabla^2 T^* \quad (2g)$$

lastly, we have to plug in  $\Pi_1 = \mathbf{u}^* = \mathbf{u} / U$  :

Rearranging (2g):

$$[(\rho c_p \mathbf{u} L)/k] \nabla T^* = \nabla^2 T^*$$

and if we plug in  $\Pi_1$ :

$$[(\rho c_p \mathbf{u}^* U L)/k] \nabla T^* = \nabla^2 T^* \quad (2h)$$

since  $U = (\alpha/L)\sqrt{(RaPr)} = (k/(\rho c_p L)) * \sqrt{(RaPr)}$

$$[(\cancel{\rho c_p} \cancel{\mathbf{u}^*} \cancel{U} \cancel{L})/\cancel{k}] [(\cancel{k}/(\cancel{\rho c_p} \cancel{L}))\sqrt{(RaPr)}] \nabla T^* = \nabla^2 T^*$$

or

$$\boxed{(\mathbf{u}^*)\sqrt{(RaPr)} \nabla T^* = \nabla^2 T^*} \quad (B)$$

The momentum equation can be manipulated similarly and obtain:

$$\boxed{\sqrt{(Ra/Pr)} (\mathbf{u}^* \nabla \mathbf{u}^*) = -\nabla p^* + \nabla^2 \mathbf{u}^* + \sqrt{(Ra/Pr)} T^*} \quad (C)$$

We cannot input these dimensionless equations straight into FIDAP, because the program does not recognize them. However, when we compare equations (A), (B), (C) with GEs (1), (2), (3) respectively, the input parameters in Ges for the FIDAP becomes:

$$\rho \sim \sqrt{(Ra/Pr)}$$

$$c_p \sim Pr$$

$$g \sim 1$$

$$\beta \sim 1$$

$$\mu \sim 1$$

$$k \sim 1$$

## Appendix D: References

- [1] Harvey, Rebecca. *The Inuit, People of the Arctic*,  
<http://www.csuchico.edu/art/contraposto/contraposto00/pages/themethod/harvey.html>
- [2] Charters. Antarctica – *Survival in Antarctica. Polar Mist Expeditions, Inc.*  
[http://www.polarmistexp.com/polarmist\\_web/antarctica/land\\_survival.html](http://www.polarmistexp.com/polarmist_web/antarctica/land_survival.html)
- [3] Wilson, J. Gonz' alex-Espada, et. al. 2001. “*The intriguing physics inside an Igloo.*”  
Science Education Department, The University of Georgia, Athens, GA 30602, USA.
- [4] Datta, A.K. 2003. *Computer-Aided Engineering: Applications to Biomedical Processes*. Dept. of Biological and Environmental Engineering, Cornell University, Ithaca, New York.
- [5] Bells Alaska Guide. 2001. *Climate*. Bells Alaska,  
<http://www.bellsalaska.com/myalaska/climates.html>
- [6] Elert. Glenn. 1998-2003. *Sensible Heat*. Hypertextbook,  
<http://www.hypertextbook.com/physics/thermal/heat-sensible/>
- [7] Kauffman, Brian. 1998. *List of Physical constants*. National Center for Atmospheric Research, <http://www.cgd.ucar.edu/csm/models/cpl/cp14.0/doc9.html>
- [8] Dyster, SJ. 2001. *Standard Properties in ADMS3-1*. Cambridge Environmental Research Consultants, [http://www.cerc.co.uk/software/pubs/ADMS3-1TechSpec/P04\\_05.pdf](http://www.cerc.co.uk/software/pubs/ADMS3-1TechSpec/P04_05.pdf)
- [9] Datta, A.K. 2002. *Biological and Bioenvironmental Heat and Mass Transfer*. Marcel Dekker, Inc., New York, NY.

(Some sites do not have authors, so the company that made the website was cited)